The Freshwater Ciliate *Coleps hirtus* as a Model Organism for Metal and Nanoparticle Toxicity: Mixture Interactions and Antioxidant Responses

Govindhasamay R. Varatharajan , Martina Coletta , Santosh Kumar , Daizy Bharti , Arnab Ghosh , Shikha Singh , Amit C. Kharkwal , Francesco Dondero , Antonietta La Terza *

Posted Date: 22 December 2025

doi: 10.20944/preprints202512.1836.v1

Keywords: cytotoxicity; binary mixture; oxidative stress; reactive oxygen species (ROS); Toxic Unit (TU); MixTOX modeling

 doi:10.20944/preprints202512.1836.v1

Article

The Freshwater Ciliate *Coleps hirtus* as a Model Organism for Metal and Nanoparticle Toxicity: Mixture Interactions and Antioxidant Responses

Govindhasamay R. Varatharajan [1,2], Martina Coletta [1], Santosh Kumar [3], Daizy Bharti [1,3], Arnab Ghosh [3], Shikha Singh [4], Amit C. Kharkwal [4], Francesco Dondero [5] and Antonietta La Terza [1,*]

[1] School of Biosciences and Veterinary Medicine, University of Camerino, Via Gentile III da Varano, 62032 Camerino (MC), Italy

[2] Faculty of Biology, Shenzhen MSU-BIT University, International University Park Road, Dayun New Town, Longgang District, Shenzhen 518172, China

[3] Zoological Survey of India, Prani Vigyan Bhawan, M-Block, New Alipore, Kolkata-700 053, India

[4] Amity Institute of Microbial Technology, Amity University Uttar Pradesh (AUUP), Noida 201313, India

[5] Department of Science and Technological Innovation (DISIT), University of Eastern Piedmont, Viale Michel 11, 15121 Alessandria, Italy

* Correspondence: antonietta.laterza@unicam.it; Tel.: +390737403224

Abstract

Heavy metals (HMs) and metal-oxide nanoparticles (NPs) frequently co-occur in freshwater systems, yet their combined effects on microbial predators remain poorly understood. Here, the freshwater ciliate *Coleps hirtus* was used to evaluate the cytotoxicity of single and binary mixtures of HMs (Cd, Cu, Zn) and NPs (ZnO, CuO, TiO_2, SiO_2), and to characterize associated antioxidant responses. Acute toxicity was assessed after 24 h by estimating LC_{20} and LC_{50} values, while mixture toxicity for Cd + Zn and Cd + ZnO was analyzed using the Toxic Unit approach and the MixTOX framework. Non-enzymatic (total phenolic content, DPPH, HRSA) and enzymatic (CAT, GST, GPx, SOD) antioxidants were quantified as sub-lethal biomarkers. HMs were markedly more toxic than NPs, with a toxicity ranking of Cu > Cd >> Zn, whereas NPs followed ZnO > CuO >> TiO_2 >> SiO_2. Cd + Zn mixtures showed predominantly antagonistic or non-interactive effects, while Cd + ZnO mixtures exhibited strong, dose-ratio–dependent synergism. Exposure to HMs and NPs induced significant and often coordinated changes in antioxidant biomarkers, with binary mixtures eliciting stronger responses than single contaminants. These results demonstrate that *C. hirtus* is sensitive to both HMs and metal-oxide NPs and can discriminate among different mixture interaction types. The combination of clear toxicity patterns and robust antioxidant responses supports the use of *C. hirtus* as a promising bioindicator for freshwater environments impacted by HMs and emerging metal-based nanomaterials.

Keywords: cytotoxicity; binary mixture; oxidative stress; reactive oxygen species (ROS); Toxic Unit (TU); MixTOX modeling

1. Introduction

An ecosystem contains various types of organic and inorganic pollutants, with heavy metals (HMs) and nanoparticles (NPs) being the most prevalent and persistent. Heavy metals such as Cd, Cu, and Zn cannot be degraded and tend to accumulate in sediments and aquatic food webs, originating from both natural processes (e.g., rock weathering, volcanic activity) and numerous human activities including mining, metallurgy, agriculture, and urban runoff [1–3]. In recent years, environmental contamination has become more complex due to the widespread use of engineered

 doi:10.20944/preprints202512.1836.v1

nanomaterials [4–6] Metal-based nanoparticles (NPs) (e.g., ZnO, CuO, TiO_2, SiO_2), widely incorporated into cosmetics, sunscreens, coatings, textiles, and medical products, enter aquatic systems through wastewater discharge and surface runoff [7–9]. Their small size and high reactivity can modify transport, dissolution, and biological uptake compared to bulk metals, potentially altering toxicity profiles. As a result, aquatic organisms are increasingly exposed to mixtures of dissolved metals and metal-oxide nanoparticles, creating new ecotoxicological scenarios that require sensitive model organisms for assessment [10].

Research into the interaction between microorganisms, especially ciliates, and HMs and NPs is currently a trending topic. Ciliates, in particular, play a crucial role in degrading organic matter and/or toxic pollutants in freshwater, soil, and sediments. They are also widely distributed globally and have environmental utility, being used in biomonitoring environmental pollution [11] and used as a bioindicator organism [12]. However, studies on the interaction between HMs and NPs in ciliated protozoa are limited compared to available data from other eukaryotic microorganisms such as yeast, fungi, and microalgae. Several ciliate species have been used as test organisms to analyze the cytotoxic effects of heavy metals and nanoparticles on cellular growth [13–20]. Most of these investigations focus on classical model ciliates, whereas species belonging to other taxonomic groups, with distinct morphologies, ecologies, and stress-response strategies, remain insufficiently explored.

In this context, *Coleps hirtus* is of particular interest. *Coleps hirtus* is cosmopolitan in distribution and a widely studied freshwater ciliate in the protostomatid group, employed for its broad ecological tolerance and feeding flexibility [21,22]. The species measures approximately 50 × 25 µm and possesses a barrel-shaped body armored with calcified plates arranged in 15–16 longitudinal rows, with a single long caudal cilium; the oral aperture lies at the anterior end (Figure 1). It feeds on bacteria, algae, flagellates, other ciliates, and even metazoan tissue (e.g., rotifers, crustaceans, zebrafish), making it both histophagous and scavenging [21,23]. *Coleps hirtus* may also exhibit cannibalistic behavior, forming coordinated pack-hunting groups [24]. To support its carnivorous feeding, it possesses specialized extrusomes concentrated around the oral region [21,25,26]. Owing to its robust morphology, chemically active extrusomes, and flexible feeding strategies, *Coleps hirtus* serves as a powerful model organism for studying predator–prey interactions, morphological defenses, and cellular responses to environmental pollutants, including HMs and NPs.

Despite these advantageous biological traits, the ecotoxicological responses of *Coleps hirtus* have never been characterized. In particular, no data exist regarding its sensitivity to single or combined exposures to HMs and NPs, nor on the antioxidant and cytotoxic biomarker patterns that might support its use as a bioindicator. This gap is notable given the species' ecological ubiquity and its potential for pollutant uptake through both passive and predatory pathways.

Many studies have shown that metals may stimulate the formation of reactive oxygen species (ROS) in microorganisms [27–29]. These ROS can cause damage to biomolecules such as DNA, proteins, and lipids, as well as disrupt redox homeostasis [30], leading to oxidative stress if not controlled by cellular antioxidant defenses. Uncontrolled oxidative stress can result in severe damage to cells, including diseases, aging, and cell death by necrosis and/or apoptosis [31]. Involvement of antioxidant enzymes is an important defense mechanism to protect organisms from oxidative stress. These enzymes include catalase (CAT), glutathione S-transferase (GST), glutathione peroxidase (GPx), superoxide dismutase (SOD), and non-enzymatic assays such as total phenolic content, DPPH scavenging activity, and HRSA assay. Induction of these antioxidant enzymes in response to metals has been reported in many organisms [32–34]. Because these biomarkers respond rapidly to environmental stressors, they represent powerful tools for detecting early physiological impairment in aquatic microorganisms.

Ecotoxicological bioassays to detect or evaluate HMs and NPs toxicity have been conducted using freshwater ciliates [20,22,35–38]. However, none of these studies has examined *Coleps hirtus*, and it remains unknown whether this species' unique biology influences its sensitivity to HMs and NPs exposure. Determining its cytotoxic and antioxidant responses is therefore essential for evaluating its potential as a bioindicator species for contaminated habitats.

 doi:10.20944/preprints202512.1836.v1

In this study, our main objective was to evaluate the cytotoxic effects of single and bimetallic mixtures of HMs (Cd, Zn, Cu) and NPs (ZnO, CuO, TiO_2, and SiO_2) on a representative freshwater ciliate species, *Coleps hirtus*, and to characterize its antioxidant responses under these stressors. We aimed to demonstrate the suitability of this species as a bioindicator of habitats polluted by HMs and NPs and to evaluate its antioxidant responses as an effective biomarker for environmental monitoring. Specifically, we quantified 24 h LC_{20} and LC_{50} values, analyzed binary mixture interactions using the Toxic Unit (TU) and MixTOX frameworks [39], and measured key enzymatic and non-enzymatic antioxidant responses. By integrating toxicity metrics, mixture effects, and biomarker activation, we also assessed whether *Coleps hirtus* possesses the sensitivity and mechanistic responsiveness required to serve as a reliable freshwater bioindicator species.

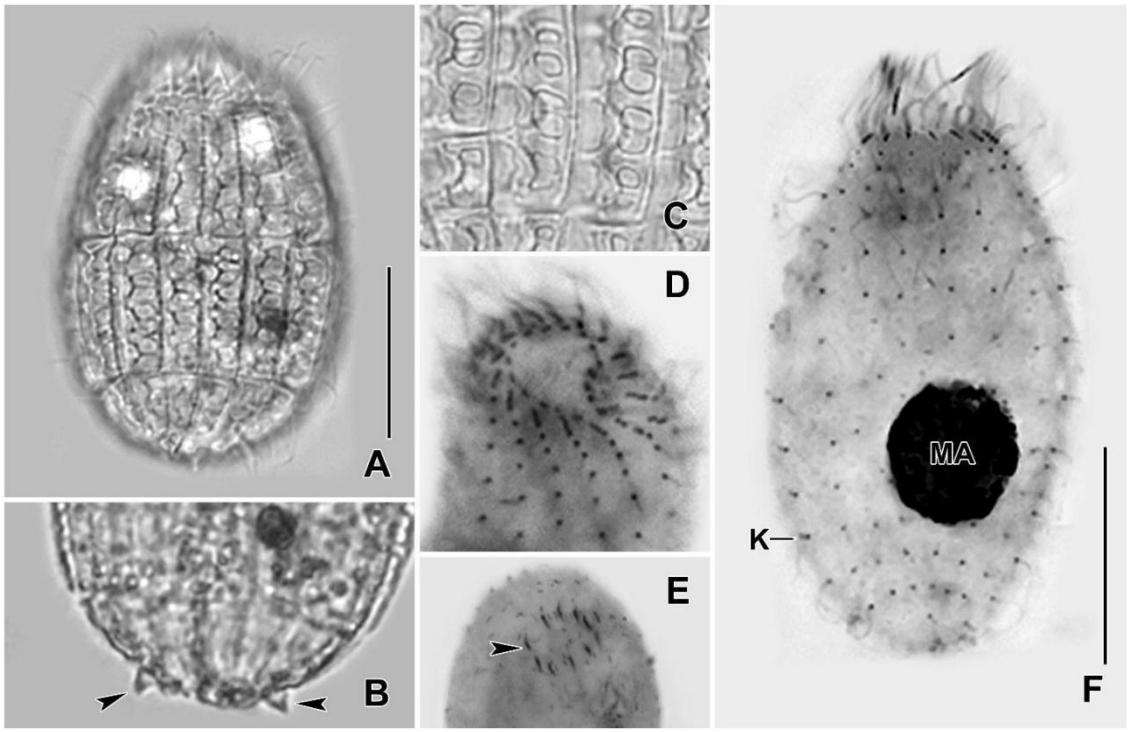

Figure 1. Photomicrographs of *Coleps hirtus* from life (A–C) and after protargol impregnation (D–F). (A) Specimen showing the body shape. (B) Arrowheads indicate the spines present at the posterior body end. (C) Segment showing the shape and arrangement of windows in the calcified plates. (D) Segment showing the oral ciliature. (E) Presence of extrusomes (arrowhead) in the oral region. (F) Specimen showing kinety rows. K, Kinety row; MA, Macronuclear nodule. Scale bars: 20 μm.

2. Materials and Methods

2.1. Ciliate Strain and Culture Conditions

The experimental organism used in our study was the freshwater ciliate *Coleps hirtus* isolated from the Sentino river (Genga, AN, Italy) (Figure 1). *C. hirtus* was grown in Salt Basel Medium (SMB) [40] at the temperature of 18 ± 1 °C. Cells were kept in the dark and were fed with green algae *Chlorogonium elongatum*. The algae *C. elongatum* was grown in Jaworski's Medium (JM) [41] at the temperature of 18 ± 1 °C. All assays were conducted using exponentially growing cells to ensure comparable metabolic states across treatments.

2.2. Metal Salts and NPs Stock Preparation

For the ecotoxicological assays, analytical grade pure chemicals (purity ≥ 99%) were used as source of metal ions and NPs: cadmium chloride (anhydrous $CdCl_2$), zinc sulphate heptahydrate

 doi:10.20944/preprints202512.1836.v1

($ZnSo_4.7H_2O$) and copper (II) sulphate pentahydrate ($CuSo_4.5H_2O$), zinc oxide (ZnO) (nanopowder < 100 nm particle size), titanium (IV) oxide (TiO_2) (mixture of rutile and anatase nanopowder, < 100 nm particle size (BET), 99.5% trace metals basis), silicon dioxide (SiO_2) (nanopowder, 10-20 nm particle size (BET), 99.5% trace metals basis), copper (II) oxide (CuO) (nanopowder, <50 nm particle size (TEM) from Sigma (Milan, Italy). Stock solutions of HMs (0.1 M) and NPs (1 M) were prepared in SMB (pH 7). Working solutions were freshly prepared before each experiment at the following nominal concentrations: 0 – 7 mg Cd/l, 0 – 4 mg Cu/l 0 – 50 mg Zn/l, 10 – 150 mg ZnO/l, 1 – 10 mg CuO/l, 500 – 8000 mg TiO_2/l and 1000 – 15000 mg SiO_2/l. NP stock suspensions were vortexed and briefly sonicated (5–10 min, 40 kHz) prior to dilution to minimize aggregation [42].

2.3. Single HMs and NPs Toxicity Tests at 24 h

Preliminary range-finding tests with *C. hirtus* were conducted to identify concentration ranges producing 0-100% mortality for each HM and NP. Based on these preliminary tests, 5–7 concentrations were selected for the final acute toxicity tests. Assays were carried out in 3-well depression glass slides (1 ml final volume). One hundred cells from exponentially growing cultures were transferred into each well containing SMB with the appropriate test concentration. The setup was covered to prevent evaporation and incubated for 24 h in a humid chamber at 18 ± 1 °C in the dark, without feeding. After the 24 h of exposure, mortality was assessed using a stereomicroscope (20–40x magnification). Cells were scored as dead when absent (lysis) or immobile and unresponsive to gentle mechanical stimulation with the tip of the micropipette. For each concentration, three replicate wells (n = 3) were used. The percentages of mortality were calculated and used to estimate LC_{20} and LC_{50} values by logit–log regression. Viability tests were performed using the Trypan Blue (TB) exclusion method, according to Strober [43].

2.4. Binary Mixture Toxicity Tests (Cd + Zn, Cd + ZnO) at 24 h

Binary mixtures were tested for Cd + Zn and Cd + ZnO using the Toxic Units (TU) according to Sprague (1970) [44]. For each toxicant, 1 TU was defined as the 24 h LC_{50} determined in the single-exposure tests. Mixtures were prepared by combining the two chemicals at fixed TU ratios, and total mixture concentrations of 0.5, 0.75, 1.0, 1.25, 1.5, 1.75, and 2.0 TUs were tested. The total TU of each mixture was calculated as the sum of the TUs contributed by each component. Expected mortality for each TU combination was obtained from the single-metal concentration–response curves, by summing the mortalities corresponding to the TU contribution of each metal in the mixture. For each mixture, observed and expected mortalities were compared. Interactions were classified as synergistic when the observed mortality was significantly higher than the expected value, antagonistic when the observed mortality was significantly lower than the expected value, and as no interaction when no significant deviation from the expected mortality was detected ($p > 0.05$). These TU-based interaction patterns were later complemented and refined by MixTOX modeling (Paragraph 2.8).

2.5. Sample Preparation for Antioxidant Analyses

For antioxidant and enzyme analyses, *C. hirtus* cells were exposed for 24 h to selected concentrations of single HMs/NPs and binary mixtures. For each treatment, 2000 cells mL^{-1} from logarithmic-phase cultures were transferred into Petri dishes (10 mL volume) containing SMB with the desired HM/NP concentration or mixture. For single exposures, 0.25, 0.5, 0.75, and 1 TU of Cd, Zn, and ZnO were used. For binary mixtures, sublethal combinations (≤ 50% mortality) were chosen based on acute toxicity data. In total, nine combinations of Cd + Zn (0.25+0.25, 0.5+0.25, 0.25+0.5, 0.75+0.25, 0.5+0.5, 0.25+0.75, 1+0.75, 0.5+1, 0.75+0.75 TUs) and six of Cd + ZnO (0.25+0.25, 0.5+0.25, 0.25+0.5, 0.75+0.25, 0.5+0.5, 1+0.25 TUs) were used for biomarker measurements. After 24 h, cells were separated from the medium by gentle centrifugation (4000 rpm, 10–15 min). Pellets were washed in distilled water (1000 rpm, 2–3 min) and resuspended in 1 mL of 50 mM phosphate buffer (pH 7.0).

 doi:10.20944/preprints202512.1836.v1

Cells were homogenized with a Teflon homogenizer for 4–5 min in the same buffer, and the homogenate was centrifuged at 4000 rpm for 30 min. The supernatant containing intracellular components was collected and stored at –20 °C until analysis. All antioxidant and enzyme assays were performed following Ravindran et al. (2012) [45].

2.6. Non-Enzymatic Antioxidant Assays

Three non-enzymatic antioxidant assays were applied to evaluate intracellular antioxidant activity in *C. hirtus* exposed to single and binary mixtures of HMs and NPs: Total Phenolic Content (TPC), DPPH radical scavenging, and Hydroxyl Radical Scavenging Assay (HRSA).

TPC was determined using the Folin–Ciocalteu method [46] with minor modifications. Briefly, 100 µL of cell extract were mixed with 2 mL of sodium bicarbonate solution and incubated for 2 min at 18 ± 2 °C. Subsequently, 100 µL of Folin–Ciocalteu reagent were added and the samples were incubated in the dark for 30 min at 18 ± 2 °C. Absorbance was measured at λ= 725 nm using the spectrophotometer (FLUOstar Omega, BMG LABTECH, Ortenberg, Germany). Gallic acid (1mg/ml) was used as the standard to construct calibration curves, and results were expressed as gallic acid equivalents. Culture medium (without cells) was used as a control.

The DPPH scavenging activity was measured following Yildrim et al. (2001) [47] with minor modifications. 1 mM DPPH stock solution was prepared in 95% ethanol. For each assay, 800 µl of DPPH solution were added to 200 µl of sample extract, incubated for 30 min in the dark at room temperature, then centrifuged at 14,000 rpm for 5 min. The absorbance of the supernatant was measured at λ = 517 nm using a spectrophotometer (FLUOstar Omega, BMG LABTECH, Ortenberg, Germany). Ethanol (95%) was used as control, and Butylated Hydroxy Anisole (BHA) was used as a reference antioxidant. Scavenging activity (%) was calculated using the following formula:

$$DPPH\ scavenging\ (\%) = \frac{control\ absorbance - extract\ absorbance}{control\ absorbance} \times 100$$

HRSA was assessed using the Fenton reaction based assay following Kunchandy & Rao (1990) [48] and Ravindran, et al. (2012) [45] with minor modifications. Hydroxyl radicals were generated in a Fe^{3+} ascorbate EDTA H_2O_2 system in 20 mM phosphate buffer (pH 7.4) containing 2.8 mM 2-deoxyribose, 100 µM $FeCl_3$, 1 mM H_2O_2, and 100 µM EDTA. From this mixture, 800 µl were transferred to test tubes, followed by 10 µl of ascorbic acid (10 mM) and 100 µl cell extract. After incubation at 37 ºC for 1 h, 1 ml of 2.8% TCA, and 1 ml of 1% TBA were added, and samples were heated at 90 °C for 15 min for colour development. After cooling, absorbance was measured at λ = 532 nm against a blank solution. Mannitol was used as the reference scavenger. The percentage of scavenging was calculated using the following formula:

$$Hydroxyl\ radical\ scavenging\ (\%) = 1 - \frac{Sample\ absorbance}{Blank\ absorbance} \times 100$$

2.7. Antioxidant Enzyme Assays

Enzymatic antioxidant activities (CAT, GST, GPx, SOD) were measured in the same extracts used for non-enzymatic assays.

CAT activity was determined according to Beers & Sizer (1952) [49] as adapted by Ravindran et al. (2012) [45]. The decrease in absorbance due to H_2O_2 decomposition was monitored at λ =240 nm in a reaction mixture containing 0.036% H_2O_2 and 100 µL of sample in phosphate buffer. One unit of CAT activity was defined as the amount of enzyme decomposing 1 mM H_2O_2 min^{-1} mg^{-1} protein at pH 7.0 and 25 °C.

GST activity was measured by following the conjugation of reduced glutathione (GSH) with 1-chloro-2,4-dinitrobenzene (CDNB) at λ =340 nm [50]. One unit of GST activity was defined as the amount of enzyme conjugating 10 nmol of CDNB with GSH per min at 25 °C.

GPx activity was measured using guaiacol as substrate, following Ravindran et al. (2012) [45]. The formation of tetraguaiacol was monitored at λ = 436 nm, and activity was expressed as units per

 doi:10.20944/preprints202512.1836.v1

mL of extract. One unit is defined as the amount of enzyme which catalyses the conversion of 1 mmol of hydrogen peroxide per minute.

SOD activity was assayed by monitoring the inhibition of NBT reduction at λ =560 nm, according to standard protocols [51]. One unit of SOD activity was defined as the amount of enzyme required to inhibit NBT reduction by 50% under the assay conditions.

2.8. Statistical Analysis and MixTOX Modeling

Statistical analyses were performed using the InfoStat software (v. 2012) (http://www.infostat.com.ar.) [52]. Mixture-toxicity modelling was conducted with the MixTOX tool of Jonker et al. [39], implemented in Microsoft® Excel. LC_{20} and LC_{50} values for single HMs and NPs were estimated by logit–log regression using log-transformed concentrations and logit-transformed mortality proportions. Differences among treatments in mortality and biomarker responses were evaluated by one-way ANOVA followed by Bonferroni post hoc tests, with $p < 0.05$ considered statistically significant. Pearson correlation coefficients (R) were calculated to determine relationships among antioxidant endpoints.

Mixture toxicity data for Cd + Zn and Cd + ZnO were further analyzed by comparing the fit of Concentration Addition (CA) and Independent Action (IA) reference models, together with deviation functions describing synergism/antagonism (S/A), dose-level dependence (DL), and dose-ratio dependence (DR). Model performance was assessed through goodness-of-fit (R^2) and χ^2 tests.

3. Results

3.1. Cytotoxicity of Single HM and NP after 24 h of Exposure

To assess the toxic effects of HMs and NPs on the population growth of the ciliate *C. hirtus*, we performed acute 24 h exposure assays with the metals Cu, Cd, Zn and with the NPs ZnO, CuO, TiO_2, and SiO_2. The toxicity ranking for HMs at 24 h was Cu > Cd >> Zn, confirming that Cu was the most toxic element, whereas Zn was the least toxic. For NPs, the toxicity ranking at 24 h was ZnO > CuO >> TiO_2 >> SiO_2. During single-metal exposures, *C. hirtus* showed higher resistance to Zn than to Cu at 24 h. Regarding NPs, the cells were highly tolerant to SiO_2, with no mortality observed at the highest tested concentrations, and relatively tolerant to TiO_2, which is consistent with the much higher LC values for these NPs.

The 24 h LC_{20} and LC_{50} values for HMs and NPs, obtained by binomial logit regression, are summarised in Table 1. For HMs, LC_{50} values were: 1.62 mg L^{-1} for Cu, 2.75 mg L^{-1} for Cd, and 20.42 mg L^{-1} for Zn. For NPs, LC_{50} values were markedly higher: 447.83 mg L^{-1} for CuO, 356.18 mg L^{-1} for ZnO, and 12.87 g L^{-1} for TiO_2, while SiO_2 produced no effects up to 60.08 g L^{-1}. A similar trend was observed for LC_{20} values with heavy metals showing much lower effective concentrations than NPs (Table 1). Overall, the data demonstrate that Cu, Cd, and Zn were markedly more toxic than ZnO, CuO, and TiO_2, whereas SiO_2 was essentially non-toxic under the conditions tested. During exposure to either HMs or NPs, *C. hirtus* cells frequently lost their characteristic barrel-shaped morphology, displayed abnormal swimming behavior, and some became rounded and immobile, particularly at higher concentrations. Based on these acute toxicity patterns, ZnO was selected as the representative NP for subsequent mixture and biomarker analyses, because it combined clear, dose-dependent toxicity with a concentration range that allowed the collection of sub-lethal samples. In contrast, CuO did not provide a sufficiently broad sub-lethal window for reliable physiological assays, whereas TiO_2 and SiO_2 showed very limited or no toxicity under comparable conditions.

Table 1. 24 h LC_{20} and LC_{50} values for HMs and NPs in *Coleps hirtus* from logit model analysis.

S. No:		Parameter	Estimate (± SE)	95% Confidence Interval	R^2
			Heavy Metals		
1	Cu	LC_{20}	0.87 ± 0.05	0.77 - 0.97	0.997

 doi:10.20944/preprints202512.1836.v1

		LC_{50}	1.62 ± 0.04	1.55 – 1.69	
2	Zn	LC_{20}	8.26 ± 0.68	6.93 – 9.59	0.987
		LC_{50}	20.42 ± 0.89	18.68 – 22.16	
3	Cd	LC_{20}	1.47 ± 0.08	1.32 – 1.62	0.994
		LC_{50}	2.75 ± 0.06	2.63 – 2.87	
			Nanoparticles		
1	CuO	LC_{20}	256.45 ± 15.32	226.43 – 286.47	0.996
		LC_{50}	447.83 ± 11.94	424.43 – 471.23	
2	ZnO	LC_{20}	138.72 ± 9.85	119.41 – 158.03	0.993
		LC_{50}	356.18 ± 16.32	324.19 – 388.17	
3	TiO_2	LC_{20}	6487.15 ± 462.25	5581.14 – 7393.16	0.995
		LC_{50}	12879.33 ± 405.67	12084.22 – 13679.44	
4	SiO_2	LC_{20}	Up to 60080 mg L^{-1} there is no effects to the cells		
		LC_{50}			

Note: concentrations are in mg L^{-1}.

3.2. Cytotoxicity of Binary Mixtures (Cd + Zn and Cd + ZnO) after 24 h of Exposure

Building on the acute toxicity patterns described above, binary mixture experiments were carried out for Cd + Zn and Cd + ZnO, using ZnO as the representative NP in combination with Cd. This design allowed a direct comparison between an ionic-metal mixture (Cd + Zn) and a metal–NP mixture (Cd + ZnO).

3.2.1. Toxic Unit (TU) Approach

The toxicity of binary mixtures was evaluated for Cd + Zn and Cd + ZnO using the TU concept. For each pair, mixtures were prepared at total concentrations ranging from 0.5 to 2 TU, with the contribution of each toxicant expressed as a fraction of its single-metal LC_{50} (1 TU). The observed and expected mortalities are reported in Tables 2 and 3.

In the Cd + Zn mixture at 24 h, interactions were predominantly antagonistic (7 antagonistic combinations), with only 4 synergistic ones and 4 combinations showing no significant difference between observed and expected mortality (Table 2). This pattern indicates that, in most cases, the presence of Zn tended to reduce the toxicity expected from Cd and vice versa. In contrast, the Cd + ZnO mixture at 24 h showed a completely different behavior. Almost all combinations exhibited clear synergistic effects (i.e., observed mortality was much higher than expected from additivity) (Table 3). Only the highest total concentration (2 TU, 1 + 1) showed no significant deviation from expected mortality. Thus, Cd substantially enhanced ZnO toxicity across a wide range of TU combinations.

Table 2. Observed and predicted cytotoxicity (% mortality) of *Coleps hirtus* to different mixtures of $CdCl_2$ + $ZnSo_4$ after 24 h exposition.

$CdCl_2$ + $ZnSo_4$ Total TU[a]	**Concentrations (TU)[a] for each compound**		**Obtained Cytotoxicity[b]**	**Expected Cytotoxicity**	**Interaction type**
	$CdCl_2$	**$ZnSo_4$**			
0.5	0.25	0.25	13.00 ± 3.04	15 ± 2.3	Not significant different
0.75	0.5	0.25	27.11 ± 1.62	29 ± 2.7	Not significant different
0.75	0.25	0.5	20.89 ± 1.27	26 ± 2.7	Antagonism
1	0.75	0.25	49.56 ± 2.60	46 ± 2.8	Synergism
1	0.5	0.5	34.00 ± 1.22	40 ± 2.8	Antagonism
1	0.25	0.75	35.44 ± 3.28	38 ± 2.8	Not significant different
1.25	0.75	0.5	42.56 ± 1.33	57 ± 2.6	Antagonism
1.25	0.5	0.75	56.67 ± 2.60	52 ± 2.6	Synergism
1.25	1	0.25	55.00 ± 2.80	62 ± 2.5	Antagonism
1.25	0.25	1	66.89 ± 2.52	53 ± 2.6	Synergism

 doi:10.20944/preprints202512.1836.v1

1.5	0.5	1	72.67	±	2.35	67	±	2.3	Synergism
1.5	0.75	0.75	53.00	±	1.00	69	±	2.3	Antagonism
1.5	1	0.5	60.33	±	1.58	73	±	2.2	Antagonism
1.75	1	075	81.00	±	2.12	85	±	1.7	Antagonism
1.75	0.75	1	87.00	±	2.74	84	±	1.7	Not significant different
2	1	1	96.56	±	2.60	100	±	0.3	Not significant different

[a]Toxic Units, mg L^{-1}. [b] % mortality ± standard deviation.

Table 3. Observed and predicted cytotoxicity (% mortality) of *Coleps hirtus* to different mixtures of $CdCl_2$ + ZnO after 24 h exposition.

$CdCl_2$ + ZnO Total TU[a]	**Concentrations (TU)[a] for each compound**		**Obtained Cytotoxicity[b]**			**Expected Cytotoxicity**			**Interaction type**
	$CdCl_2$	**ZnO**							
0.5	0.25	0.25	42.33	±	1.94	8	±	0.3	Synergism
0.75	0.5	0.25	51.67	±	1.87	22	±	1.0	Synergism
0.75	0.25	0.5	74.11	±	1.45	22	±	1.0	Synergism
1	0.75	0.25	67.44	±	2.46	39	±	2.1	Synergism
1	0.5	0.5	84.56	±	1.42	36	±	2.0	Synergism
1	0.25	0.75	100.00	±	0.00	36	±	2.0	Synergism
1.25	0.75	0.5	88.67	±	1.00	53	±	2.4	Synergism
1.25	0.5	0.75	100.00	±	0.00	49	±	2.4	Synergism
1.25	1	0.25	76.22	±	2.11	55	±	2.3	Synergism
1.25	0.25	1	100.00	±	0.00	53	±	2.4	Synergism
1.5	0.5	1	100.00	±	0.00	67	±	2.0	Synergism
1.5	0.75	0.75	100.00	±	0.00	66	±	2.0	Synergism
1.5	1	0.5	95.11	±	1.27	69	±	1.9	Synergism
1.75	1	075	100.00	±	0.00	82	±	1.3	Synergism
1.75	0.75	1	100.00	±	0.00	84	±	1.2	Synergism
2	1	1	100.00	±	0.00	100	±	0.2	Not significant different

[a]Toxic Units, mg L^{-1}. [b] % mortality ± standard deviation.

3.2.2. MixTOX Modeling

Binary mixture data were further analyzed with the MixTOX tool [39] using the Concentration Addition (CA) and Independent Action (IA) reference models and their deviation functions (S/A, DL, DR). The corresponding parameters and goodness-of-fit statistics are reported in Tables 4 and 5.

For the Cd + Zn mixture at 24 h, the IA model provided the best overall description of the data, explaining 93% of the variance (R^2 = 0.93), whereas CA and its deviation models explained between 88% and 91% (Table 4). No IA-based deviation model (S/A, DL, DR) significantly improved the fit compared to IA alone ($p(\chi^2) > 0.05$), indicating that Cd and Zn behaved largely as independent toxicants with modest deviations. Among CA-based models, the CA/DL (dose-level–dependent) deviation model performed relatively better and suggested some degree of antagonism at higher dose levels, consistent with the TU analysis.

For the Cd + ZnO mixture at 24 h, both CA- and IA-based basic models performed poorly unless deviation functions were included (Table 6). The CA model alone explained only 77% of the variance, whereas CA/S/A, CA/DL, and especially CA/DR models considerably improved the fit, reaching R^2 values up to 0.96. Similarly, IA alone explained only 33% of the variance, but IA/S/A, IA/DL, and particularly IA/DR reached R^2 values between 0.90 and 0.96. The best-fitting model overall was IA/DR (R^2 = 0.96), indicating strong dose-ratio–dependent synergism between Cd and ZnO.

 doi:10.20944/preprints202512.1836.v1

Table 4. Fitting results of the toxicity of the bimetallic mixture (Cd + Zn) data to the four models describing deviations from concentration addition (CA) and independent action (IA) of *Coleps hirtus* by the MixTOX tool.

C. hirtus $CdCl_2$ + $ZnSo_4$ exposures	Parameter	The Concentration Addition (CA) based module			
		CA	**S/A**	**DR**	**DL**
24 hr	*a*	–	0.487	0.087	1.829
	b	–	–	0.783	0.583
	R^2	0.88	0.90	0.90	0.91
	p (χ2) CA vs.	–	6.45E-07*	2.04E-06*	4.71E-09*
	S/A vs.	–	–	0.231	0.0002*
	Parameter	**The Independent action (IA) based module**			
		IA	**S/A**	**DR**	**DL**
24 hr	*a*	–	-0.147	-0.689	-0.047
	b	–	–	1.108	-3.925
	R^2	0.93	0.93	0.91	0.93
	p (χ2) IA vs.	–	0.331	0.343	0.604
	S/A vs.	–	–	0.274	0.802

24 hr: 24 hour exposure period; CA: the concentration addition model; IA: the independent addition model; *a* and *b*: interaction parameters; S/A: the model describing synergy or antagonism in relation to the reference model has one interaction parameter (*a*); DR: the model describing dose ratio–dependent deviations from the reference model has two interaction parameters (*a* and *b*); DL: the model describing dose level–dependent deviations from the reference model has two interaction parameters (*a* and *b*); R^2: the coefficient of determination; *p* (χ2): the outcome of the likelihood ratio test; vs.: versus, which was used to show comparison between two models; –: not applicable. *: Significant at the 5% significant level.

Table 5. Fitting results of the toxicity of the binary mixture (Cd + ZnO) data to the four models describing deviations from concentration addition (CA) and independent action (IA) of *Coleps hirtus* by the MixTOX tool.

C. hirtus $CdCl_2$ + ZnO exposures	Parameter	The Concentration Addition (CA) based module			
		CA	**S/A**	**DR**	**DL**
24 hr	*a*	–	-1.986	-5.702	-0.820
	b	–	–	7.118	-1.705
	R^2	0.77	0.93	0.96	0.93
	p (χ2) CA vs.	–	2.2E-80*	5.5E-100*	7.99E-81*
	S/A vs.	–	–	8.36E-23*	0.003*
	Parameter	**The Independent action (IA) based module**			
		IA	**S/A**	**DR**	**DL**
24 hr	*a*	–	-5.629	-12.304	-7.321
	b	–	–	12.741	0.008
	R^2	0.33	0.92	0.96	0.90
	p (χ2) IA vs.	–	0.000*	0.000*	0.000*
	S/A vs.	–	–	7.75E-22*	1.03E-06*

24 hr: 24 hour exposure period; CA: the concentration addition model; IA: the independent addition model; *a* and *b*: interaction parameters; S/A: the model describing synergy or antagonism in relation to the reference model has one interaction parameter (*a*); DR: the model describing dose ratio–dependent deviations from the reference model has two interaction parameters (*a* and *b*); DL: the model describing dose level–dependent deviations from the reference model has two interaction parameters (*a* and *b*); R^2: the coefficient of determination; *p* (χ2): the outcome of the likelihood ratio test; vs.: versus, which was used to show comparison between two models; –: not applicable. *: Significant at the 5% significant level.

 doi:10.20944/preprints202512.1836.v1

Table 6. Correlation Coefficient (*R*) between single and binary mixture compound exposures of different antioxidant assays on *Coleps hirtus*.

	Single-compound treatment 24 hr		
	TPC	**DPPH**	**HRSA**
TPC	1		
DPPH	0.784	1	
HRSA	0.785	0.665	1
	Bimixture (Cd + Zn) 24 hr		
	TPC	**DPPH**	**HRSA**
TPC	1		
DPPH	0.666	1	
HRSA	0.799	0.952	1

These results show that in Cd + Zn mixtures the interaction is mostly antagonistic or close to independent, whereas in Cd + ZnO mixtures synergism is dominant, and its intensity depends on both total dose and dose ratio. For Cd + ZnO, the level of synergism tends to decrease at the highest total doses (Figure 2) but remains clearly detectable across the whole range of TU combinations.

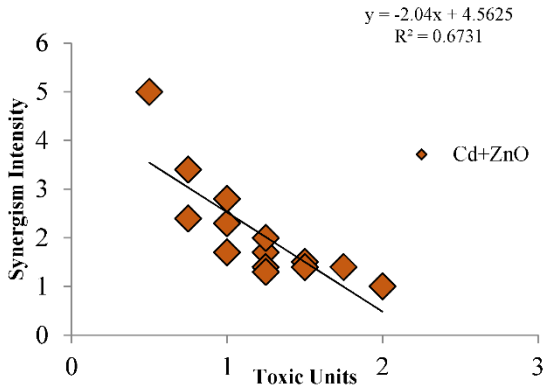

Figure 2. Intensity of synergism Vs dose level in the bimetallic mixture of Cd + ZnO at 24 hr.

3.3. Antioxidant Properties of Coleps hirtus Cell Extracts

3.3.1. Total Phenolic Content (TPC)

Phenolic compounds such as flavonoids and phenolic acids are known to be significant contributors to the antioxidant capacity of all living organisms [53]. TPC was measured in cell extracts after exposure to single-compound treatments (Cd, Zn, ZnO) and binary mixtures (Cd + Zn and Cd + ZnO) at 24 h (Figure 3). In single-compound exposures, TPC values ranged from 77.26 to 147.71 µg L^{-1} of ciliate extract. The lowest phenolic content was recorded at 1 TU ZnO, while the highest was observed at 1 TU Zn, with all differences being highly significant ($p < 0.001$; Figure 3a).

In the Cd + Zn mixture, TPC ranged between 112.86 and 173.97 µg L^{-1} at 24 h (Figure 3b). The lowest value was found in the 0.5 + 0.5 TU combination, whereas the highest TPC occurred at 0.25 + 0.75 TU (Cd + Zn), again with $p < 0.001$. In the Cd + ZnO mixture, TPC values ranged from 120.06 to 211.15 µg L^{-1} (Figure 3c). Here, the minimum was observed at 0.75 + 0.25 TU (Cd + ZnO), and the maximum at 0.25 + 0.25 TU, with highly significant differences ($p < 0.001$). Overall, TPC was higher in binary mixtures than in single-compound treatments, particularly in Cd + ZnO, suggesting that phenolic-metabolites are strongly induced under combined HM-NPs stress.

 doi:10.20944/preprints202512.1836.v1

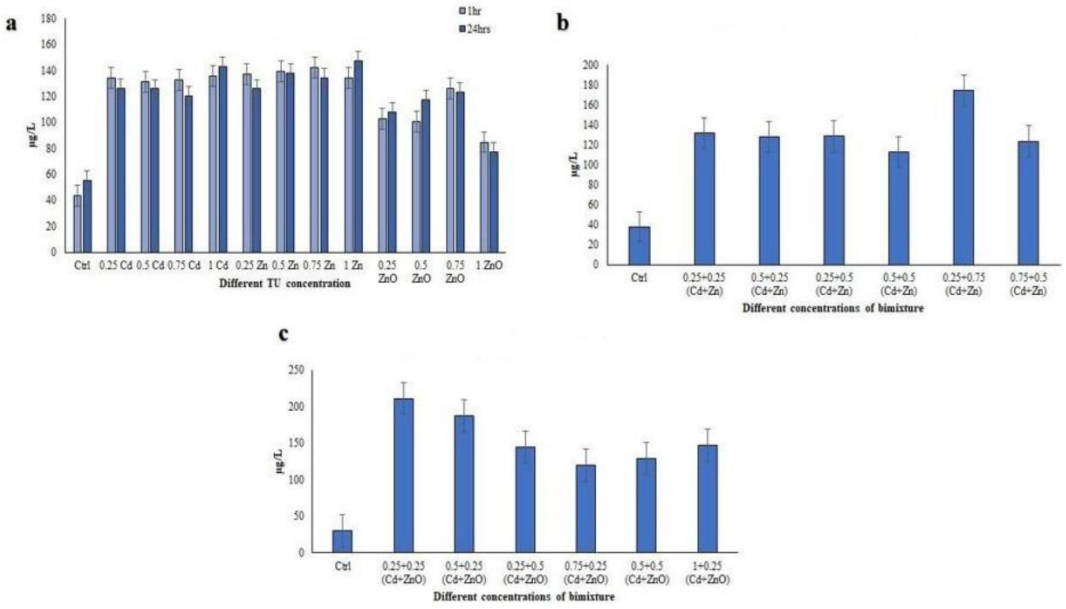

Figure 3. Total phenolic content in *Coleps hirtus* cell extracts after 24 h exposure to: individual HM (Cd, Zn) and NP (ZnO) treatments, b) Cd+Zn mixtures and c) Cd+ZnO mixtures. Results are presented as means of three replicate experiments ±SD.

3.3.2. DPPH Radical Scavenging Activity

DPPH radical scavenging activity was evaluated after 24 h exposure in cell extracts from *C. hirtus* exposed to single-compounds treatments (Cd, Zn, ZnO) and to binary mixtures (Cd+Zn and Cd+ZnO) (Figure 4). In single-compound exposures, DPPH scavenging ranged from 27.77% to 64.92% ($p < 0.001$), with the highest activity at 0.25 TU Cd and the lowest at 1 TU ZnO (Figure 4a). In the Cd + Zn mixture, DPPH scavenging activity ranged between 45.71% and 76.22% (Figure 4b). The highest value was observed at 0.25 + 0.25 TU (Cd + Zn), whereas the lowest was recorded at 0.25 + 0.75 TU (Cd + Zn), with all significant at $p < 0.001$. In the Cd + ZnO mixture, DPPH activities varied from 26.51% to 72.69% (Figure 4c). The maximum was at 0.25 + 0.25 TU (Cd + ZnO) and the minimum at 0.5 + 0.25 TU (Cd + ZnO), again with $p < 0.001$. These results indicate that exposure to binary mixtures generally enhanced DPPH scavenging compared to single-metals, particularly for low-to-intermediate TU combinations of Cd with either Zn or ZnO.

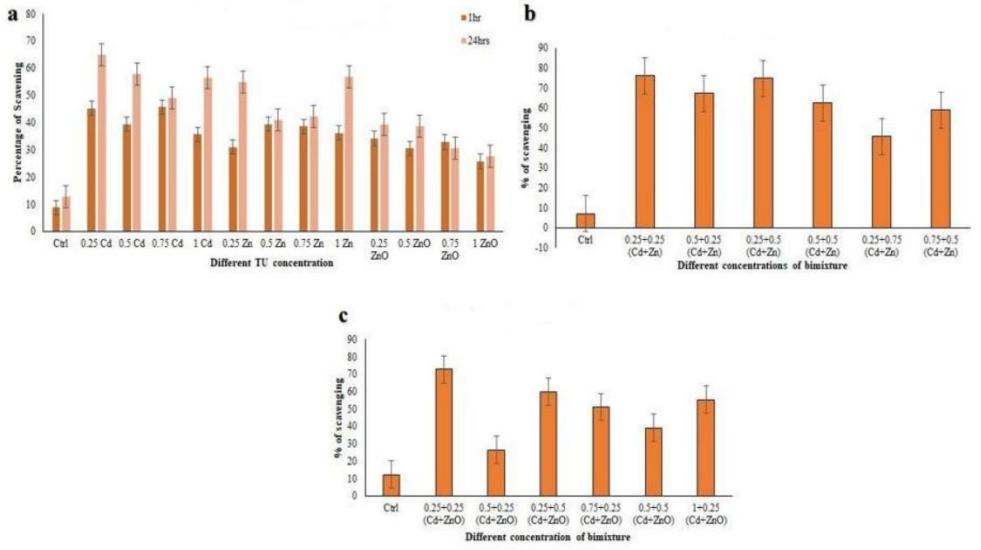

 doi:10.20944/preprints202512.1836.v1

Figure 4. DPPH scavenging activity measured in *Coleps hirtus* cell extracts after 24 h exposure to: individual HM (Cd, Zn) and NP (ZnO) treatments, b) Cd+Zn mixtures and c) Cd+ZnO mixtures. Results are presented as means of three replicate experiments ±SD.

3.3.3. Hydroxyl Radical Scavenging Activity (HRSA)

Hydroxyl radical scavenging activity (HRSA) was also determined in cell extracts after 24 h exposure (Figure 5). The ciliate extracts showed noticeable hydroxyl radical scavenging activity with increasing concentration. In single-compound treatments, HRSA ranged from 60.55% to 74.69%, with the lowest value at 0.5 TU ZnO and the highest at 1 TU Zn ($p < 0.001$; Figure 5a). In Cd + Zn mixtures, HRSA values ranged from 49.10% to 66.66% at 24 h (Figure 5b). The minimum was observed at 0.25 + 0.75 TU (Cd+Zn), with all comparisons significant ($p < 0.001$). In Cd + ZnO mixtures, HRSA ranged from 49.53% to 63.27% (Figure 5c). with the lowest value at 0.25 + 0.25 TU and the highest at 0.5 + 0.25 TU (Cd + ZnO) ($p < 0.001$). In contrast to DPPH and TPC, single-metal treatments (particularly Zn) elicited the highest HRSA values, whereas binary mixtures produced slightly lower but still elevated hydroxyl radical scavenging. This suggests that different antioxidant mechanisms and compounds may be involved in scavenging distinct ROS species.

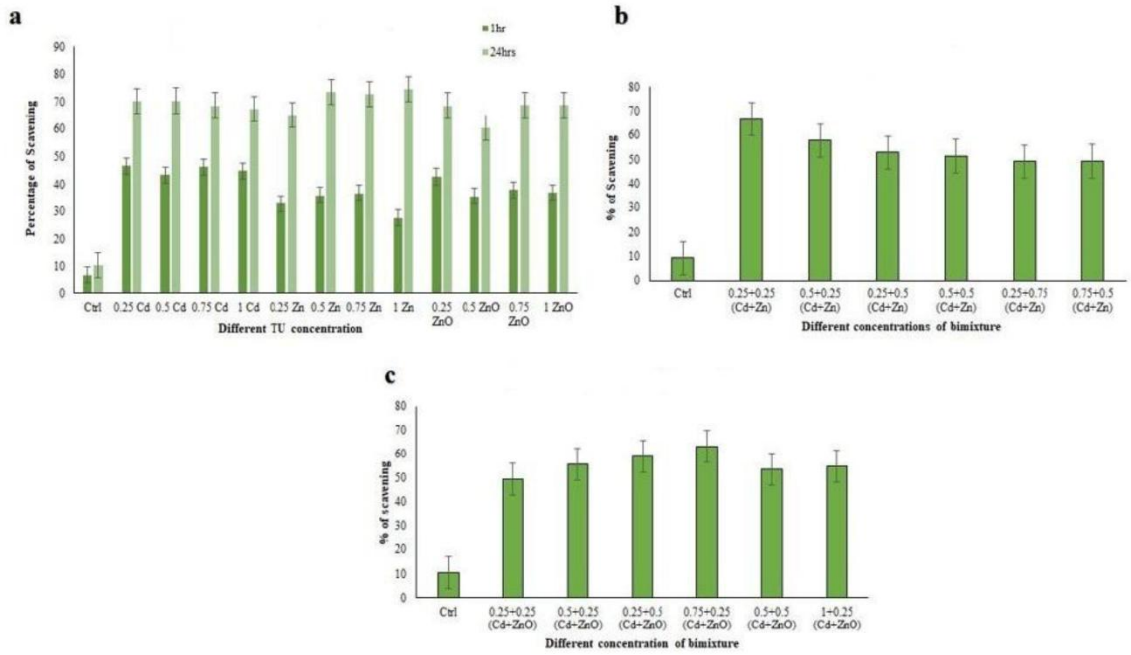

Figure 5. Hydroxyl radical scavenging activity (HRSA) measured in *Coleps hirtus* cell extracts after 24 h exposure to: individual HM (Cd, Zn) and NP (ZnO) treatments, b) Cd+Zn mixtures and c) Cd+ZnO mixtures. Results are presented as means of three replicate experiments ±SD.

3.4. Antioxidant Enzyme Activities

3.4.1. Catalase (CAT) Assay

CAT activity in *C. hirtus* extracts ranged from 14.84 to 29.91 U mL^{-1} after 24 h single-compound exposure (Figure 6a). The lowest activity was detected at 0.25 TU ZnO, whereas the highest was at 0.75 TU Zn. In the Cd + Zn mixture, CAT activity ranged from 35.36 to 40.41 U mL^{-1} (Figure 6b), with the minimum at 0.75 + 0.5 TU and the maximum at 0.5 + 0.5 TU (Cd + Zn). In the Cd + ZnO mixture, CAT activity varied between 37.90 and 43.12 U mL^{-1} (Figure 6c), with the lowest value at 0.25 + 0.5 TU and the highest at 0.5 + 0.5 TU (Cd + ZnO). Thus, CAT activity was consistently higher in binary mixture treatments (Cd + Zn, Cd + ZnO) than in single-compound exposures (Cd, Zn, ZnO), with the Cd + ZnO combination eliciting the strongest response.

 doi:10.20944/preprints202512.1836.v1

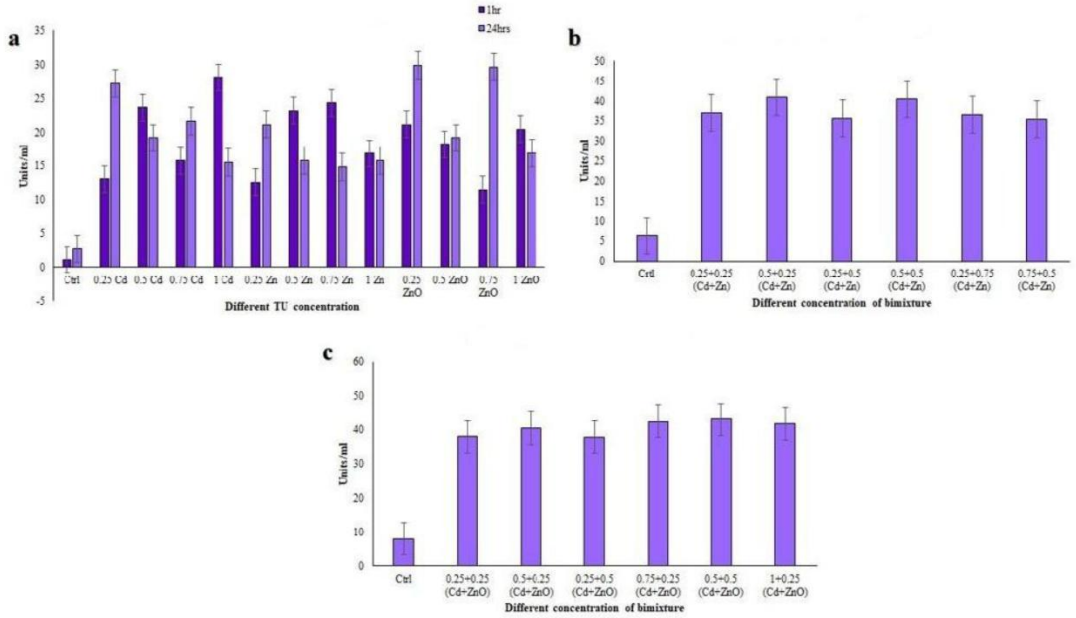

Figure 6. Catalase activity measured in *Coleps hirtus* cell extracts after 24 h exposure to: individual HM (Cd, Zn) and NP (ZnO) treatments, b) Cd+Zn mixtures and c) Cd+ZnO mixtures. Results are presented as means of three replicate experiments ±SD.

3.4.2. Glutathione S-Transferase (GST) Assay

GST catalyzes the conjugation of the reduced form of glutathione to xenobiotic substrates for detoxification purposes. GST activity in single-compound treatments ranged from 57.29 to 139.24 U mL^{-1} (Figure 7a). The lowest activity was observed at 0.5 TU Cd and the highest at 0.75 TU Zn. In the Cd + Zn mixture at 24 h, GST activity increased substantially, ranging from 361.11 to 492.03 U mL^{-1} (Figure 7b). The highest level was recorded at 0.5 + 0.5 TU (Cd + Zn) and the lowest at 0.75 + 0.5 TU (Cd + Zn). In the Cd + ZnO mixture, GST activity ranged from 163.54 to 263.54 U mL^{-1} (Figure 7c), with the minimum at 0.25 + 0.25 TU (Cd + ZnO) and the maximum at 0.5 + 0.5 TU (Cd + ZnO). These results indicate a strong induction of GST under co-exposure, especially in Cd + Zn mixtures, suggesting a key role for glutathione-dependent detoxification pathways in response to metal and nanoparticle stress.

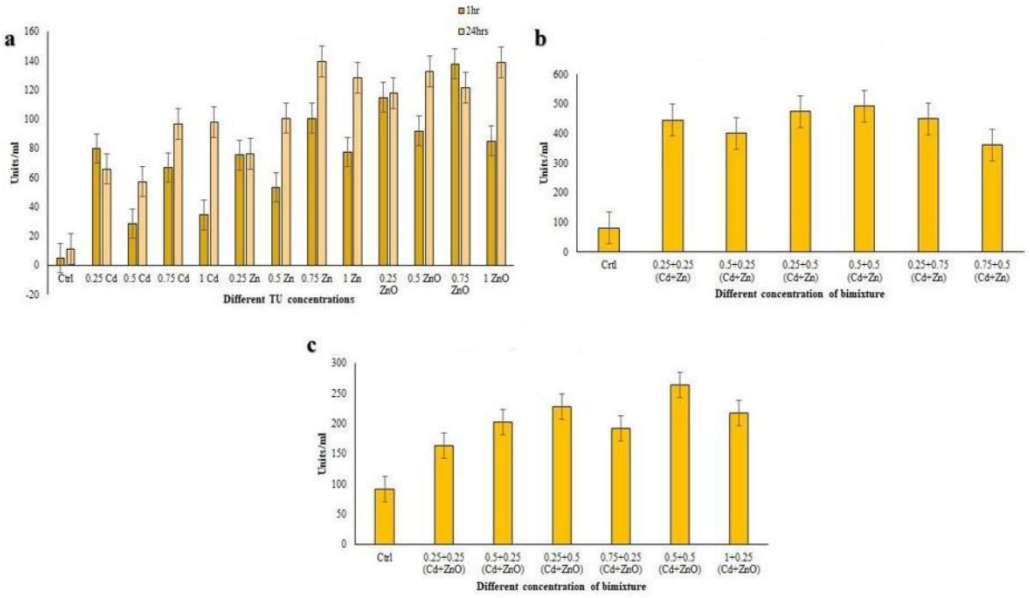

 doi:10.20944/preprints202512.1836.v1

Figure 7. Glutathione S-transferase (GST) activity measured in *Coleps hirtus* cell extracts after 24 h exposure to: individual HM (Cd, Zn) and NP (ZnO) treatments, b) Cd+Zn mixtures and c) Cd+ZnO mixtures. Results are presented as means of three replicate experiments ±SD.

3.4.3. Guaiacol Peroxidase (GPx) Assay

Peroxidases play a key role in enhancing a cell's defenses against pathogens and environmental stresses. GPx activity in single-compound treatments ranged between 0.11 and 0.23 U mL^{-1} (Figure 8a). The minimum value was recorded at 0.75 TU ZnO, and the maximum at 0.25 TU ZnO. In Cd + Zn mixtures, GPx activity increased markedly, ranging from 1.16 to 1.54 U mL^{-1} (Figure 8b). The lowest activity was observed at 0.75 + 0.5 TU and the highest at 0.25 + 0.5 TU (Cd + Zn). In Cd + ZnO mixtures, GPx activity further increased, ranging from 1.24 to 1.75 U mL^{-1} (Figure 8c), with minimum at 0.75 + 0.25 TU and maximum at 0.5 + 0.25 TU (Cd + ZnO). Overall, GPx activity was considerably higher in binary mixtures than in single-compound treatments, with Cd + ZnO producing the strongest induction, consistent with the synergistic toxicity of this mixture.

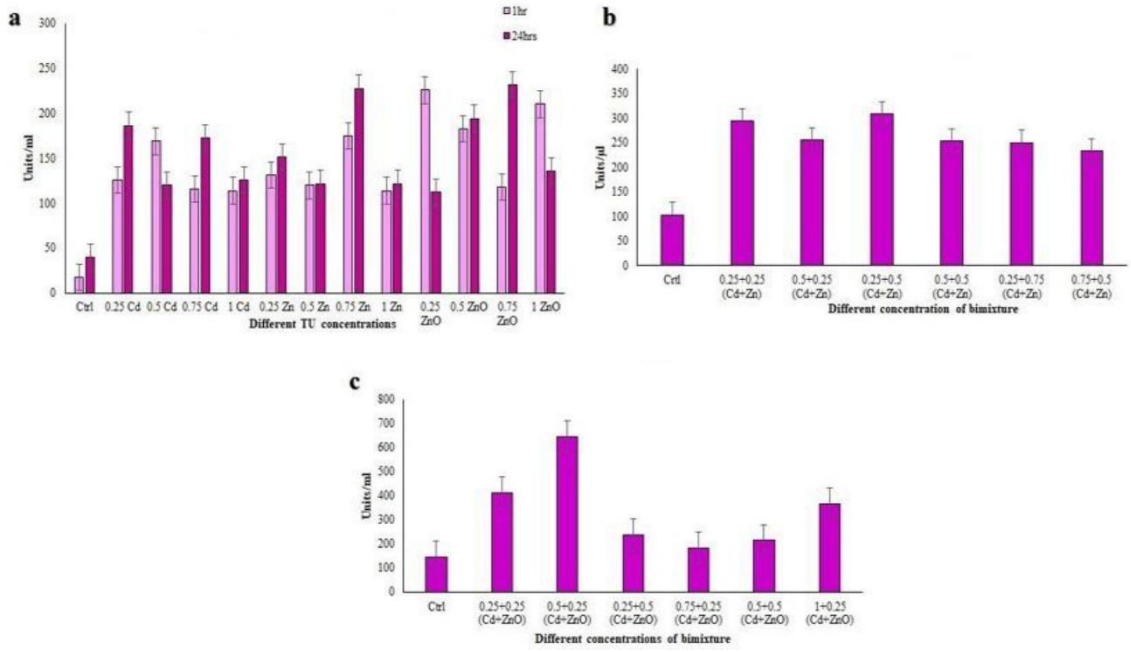

Figure 8. Guaiacol peroxidase (GPx) activity measured in *Coleps hirtus* cell extracts after 24 h exposure to: individual HM (Cd, Zn) and NP (ZnO) treatments, b) Cd+Zn mixtures and c) Cd+ZnO mixtures. Results are presented as means of three replicate experiments ±SD.

3.4.4. Superoxide Dismutase (SOD) Assay

SOD enzymes deal with the reactive oxygen species (ROS)/free radical by consecutively adding or removing an electron from the superoxide molecules it encounters, thus changing the O_2^- into one of two less damaging species: either molecular oxygen (O_2) or hydrogen peroxide (H_2O_2). Superoxide is produced as a by-product of oxygen metabolism and, if not regulated, causes many types of cell damage [54]. Due to its importance in scavenging ROS and free radicals, we evaluated SOD activity in the *C. hirtus* extracts. SOD activity in single-compound exposures ranged from 0.11 to 0.27 U mL^{-1} (Figure 9a). The highest activity was observed at 0.25 TU Cd, whereas the lowest was recorded at 0.75 TU Zn. In Cd + Zn mixtures, SOD activity increased to values between 0.44 and 0.52 U mL^{-1} (Figure 9b), with the maximum at 0.25 + 0.5 TU and the minimum at 0.75 + 0.5 TU (Cd + Zn). In Cd + ZnO mixtures, SOD activity ranged from 0.36 to 0.59 U mL^{-1} (Figure 9c), with the lowest value at 0.75 + 0.25 TU and the highest at 1 + 0.25 TU (Cd + ZnO). Thus, SOD activity was enhanced under binary exposures compared to single-metals, with the highest responses again associated with Cd + ZnO combinations.

 doi:10.20944/preprints202512.1836.v1

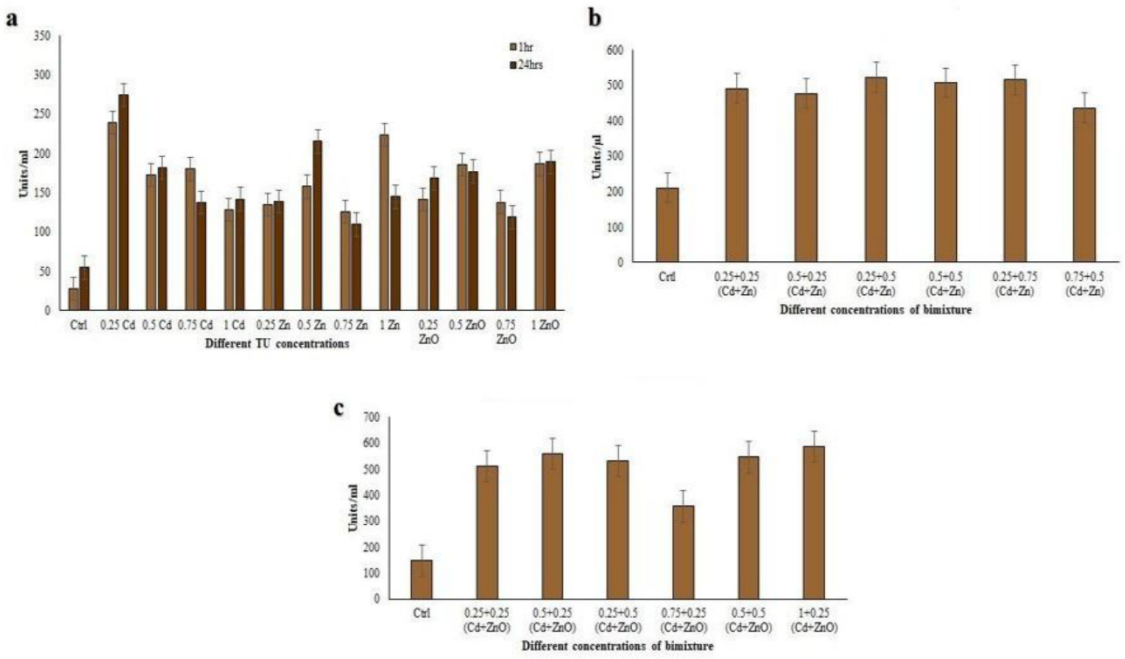

Figure 9. Superoxide dismutase (SOD) activity measured in *Coleps hirtus* cell extracts after 24 h exposure to: individual HM (Cd, Zn) and NP (ZnO) treatments, b) Cd+Zn mixtures and c) Cd+ZnO mixtures. Results are presented as means of three replicate experiments ±SD.

3.5. Correlation Analyses Among Antioxidant Responses

3.5.1. Correlations Among Non-Enzymatic Antioxidant Assays

Correlation coefficients (R) between TPC, DPPH, and HRSA are reported in Table 6. In single-compound treatments at 24 h, TPC vs. DPPH and TPC vs. HRSA showed strong positive correlations (R = 0.784 and R = 0.785, respectively), indicating that higher phenolic content was associated with higher radical scavenging capacity. DPPH vs. HRSA showed a moderate positive correlation (R = 0.665), reflecting that these assays, although related, respond to different radical species. In Cd + Zn mixtures at 24 h, TPC vs. DPPH remained moderately correlated (R = 0.666), while TPC vs. HRSA showed a strong correlation (R = 0.799). The DPPH vs. HRSA correlation increased markedly (R = 0.952), suggesting a highly coordinated antioxidant response under metal co-exposure. Overall, these patterns indicate that phenolic compounds are major contributors to antioxidant capacity in *C. hirtus*, and that their involvement becomes more tightly coupled with DPPH and HRSA under binary mixture stress.

3.5.2. Correlations Among Antioxidant Enzymes

Correlation coefficients between antioxidant enzyme activities (CAT, GST, GPx, SOD) are summarized in Table 7. In single-compound treatments at 24 h, correlations were generally weak to moderate: CAT vs. GST (R = 0.364), CAT vs. GPx (R = 0.565), CAT vs. SOD (R = 0.490), GST vs. GPx (R = 0.5848), GST vs. SOD (R = 0.151), and GPx vs. SOD (R = 0.194). These values suggest that, under single-compound exposure, each enzyme responds somewhat independently, reflecting partially distinct roles in ROS detoxification. In contrast, under Cd + Zn co-exposure, all enzymes showed very strong positive correlations: CAT vs. GST (R = 0.945), CAT vs. GPx (R = 0.884), CAT vs. SOD (R = 0.952), GST vs. GPx (R = 0.938), GST vs. SOD (R = 0.992), and GPx vs. SOD (R = 0.947). This indicates that, in the presence of both metals, antioxidant enzymes respond in a highly coordinated and interdependent manner, forming an integrated defense system. Overall, correlation analyses reveal that *C. hirtus* mounts a more synchronized antioxidant response under binary metal stress than under single-metal exposure, consistent with the higher complexity and toxicity of metal mixtures.

 doi:10.20944/preprints202512.1836.v1

Table 7. Correlation Coefficient (*R*) between single and binary mixture exposures of different antioxidant enzyme assays on *Coleps hirtus*.

	Single-compound treatment 24 hr			
	CAT	**GST**	**GPx**	**SOD**
CAT	1			
GST	0.364	1		
GPx	0.565	0.5848	1	
SOD	0.490	0.151	0.194	1
	Bimixture (Cd + Zn) 24 hr			
	CAT	**GST**	**GPx**	**SOD**
CAT	1			
GST	0.945	1		
GPx	0.884	0.938	1	
SOD	0.952	0.992	0.947	1

4. Discussion

The present study provides the first integrated assessment of cytotoxicity, mixture toxicity, and antioxidant responses to HMs and metal-NPs in the freshwater ciliate *C. hirtus*. By combining acute lethality tests with biochemical biomarkers under both single and binary exposures, we expand current knowledge on ciliate stress physiology and evaluate the potential of this species as a bioindicator of metallic pollution.

4.1. Toxicity Profiles of HMs and NPs

Previous studies have shown that freshwater ciliates tend to be more sensitive to Cu than to other heavy metals such as Cd, Zn, Pb, Ni, and Cr [13]. Our results are consistent with this general pattern: Cu was the most toxic metal for *C. hirtus* (24 h LC_{50} = 1.62 mg L^{-1}), followed by Cd (2.75 mg L^{-1}) and Zn (20.42 mg L^{-1}). This ranking agrees with observations in other ciliate species, including *Euplotes aediculatus*, *Euplotes crassus*, *Tetrahymena* spp., *Colpoda steinii*, and various soil ciliates [10,19,20,55–58], although the magnitude of LC_{50} values differs among taxa, reflecting species-specific tolerance. In our previous work, we characterized metal toxicity in *E. aediculatus* and *Rigidohymena tetracirrata* [10,55], two additional ciliates proposed as useful test organisms. When compared to those species, *C. hirtus* exhibits comparable or higher sensitivity to Cd and Zn, and a Cu sensitivity within the lower range of reported values. These features indicate that *C. hirtus* is neither unusually tolerant nor insensitive to these priority metals and can therefore detect ecologically relevant concentration ranges, which is desirable for bioindicator applications. NPs were substantially less toxic than their dissolved metal counterparts on a mass basis. ZnO and CuO exhibited intermediate toxicity, while TiO_2 and especially SiO_2 induced negligible mortality even at the highest tested concentrations. This pattern is in line with reports on other ciliates and microorganisms, where metal-oxide NPs frequently show lower acute toxicity than free metal ions and where toxicity is often linked to partial dissolution and ion release [16,17,36,57,59]. The very high LC_{50} values obtained for TiO_2 and SiO_2 are consistent with their low solubility and reactivity under the tested conditions. Overall, our data support the view that ionic forms of Cu, Cd, and Zn represent a greater acute hazard to *C. hirtus* than the metal-oxide nanoparticles studied here.

4.2. Mixture Toxicity: Antagonism in Cd + Zn vs. Synergism in Cd + ZnO

The binary Cd + Zn mixture exhibited predominantly antagonistic interactions when evaluated using the TU approach (Table 2). In most combinations, observed mortality was lower than expected, indicating that the two metals partially reduce each other's toxicity. This agrees with previous observations in fish, invertebrates, and microalgae, where Zn can mitigate Cd toxicity by competing for uptake sites or intracellular ligands [60–64]. MixTOX analysis corroborated this interpretation: the

 doi:10.20944/preprints202512.1836.v1

Independent Action (IA) model provided the best fit to the data ($R^2 = 0.93$), and inclusion of IA-based deviation terms did not substantially improve model performance (Table 4), suggesting largely independent action with modest antagonistic deviations. In contrast, the Cd + ZnO mixture displayed clear synergism over almost the entire TU range (Table 3). Here, basic CA and IA models alone did not adequately describe the data, whereas deviation models, especially IA/DR (dose-ratio–dependent deviation), significantly improved the fit (R^2 up to 0.96; Table 5). This indicates that the magnitude of synergism depends on the relative proportions of Cd and ZnO, with some dose ratios producing particularly strong combined effects. Although the underlying mechanisms were not directly investigated, several factors may contribute to this synergy: Cd-induced alterations in membrane integrity and ion homeostasis may facilitate nanoparticle interaction or uptake; ZnO dissolution dynamics may change in the presence of Cd^{2+} and other ions; and nanoparticles may act as carriers for Cd, promoting co-delivery into cells. Regardless of the exact mechanism, the strong synergistic toxicity of Cd + ZnO demonstrates that the chemical form of zinc (ionic vs. nanoparticulate) profoundly influences mixture outcomes. This has important ecotoxicological implications, as natural waters increasingly contain both dissolved metals and engineered NPs.

4.3. Antioxidant Responses as Biomarkers of Oxidative Stress

HMs and NPs are known to induce ROS generation in microorganisms, leading to oxidative damage unless counteracted by antioxidant defenses [41–51]. In *C. hirtus*, we observed clear and statistically significant changes in both non-enzymatic and enzymatic antioxidant parameters following exposure to HMs and NPs, with particularly strong responses in binary mixtures. Non-enzymatic endpoints, total phenolic content (TPC), DPPH, and HRSA, were consistently elevated in exposed cells compared with controls, and often showed higher values in mixtures than in single-metal treatments, especially in Cd + ZnO. This indicates that phenolic-like compounds and other small-molecule antioxidants are mobilized as part of the defense strategy against ROS generated by metallic stress. The strong positive correlations between TPC and both DPPH and HRSA in single-metal exposures ($R = 0.78$) and the very high DPPH–HRSA correlation under Cd + Zn mixtures ($R = 0.952$; Table 6) suggest that these assays reflect closely related aspects of the non-enzymatic antioxidant system, which becomes more tightly coordinated as stress intensifies.

Enzymatic antioxidants (CAT, GST, GPx, SOD) also showed pronounced, concentration-dependent activation. Activity levels were generally higher in binary mixtures than in single-compound exposures, with GST and SOD showing the strongest induction, particularly in Cd + Zn and Cd + ZnO treatments. This pattern points to an important role of glutathione-dependent detoxification and superoxide dismutation in the management of metal- and nanoparticle-induced oxidative stress in *C. hirtus*, consistent with observations in other protists and metazoans [45,65–69].

4.4. Coordination of Antioxidant Enzyme Responses under Mixture Stress

Beyond the magnitude of individual responses, the correlation structure among antioxidant enzymes provides insight into how *C. hirtus* organizes its defense system under different stress scenarios. In single-compound treatments, correlations among CAT, GST, GPx, and SOD were weak to moderate ($R \leq 0.58$; Table 7), suggesting that these enzymes are regulated in a relatively independent fashion and may respond to distinct ROS signals or damage types.

In contrast, under Cd + Zn co-exposure, all enzyme pairs displayed very strong positive correlations ($R \geq 0.884$), with GST–SOD approaching unity ($R = 0.992$). This indicates a shift toward a highly coordinated enzymatic response when the organism faces a more complex stressor, such as a metal mixture. Such coordination implies that the antioxidant system operates as an integrated network rather than a set of isolated pathways, and that multiple enzymes could serve as mutually reinforcing biomarkers in mixture toxicity assessments. Although correlation values for Cd + ZnO were not explicitly detailed here, the strong induction of all enzymes in that mixture is consistent with a similarly integrated response under synergistic conditions.

 doi:10.20944/preprints202512.1836.v1

4.5. Ecotoxicological Relevance of Coleps hirtus and Implications for Biomonitoring

Overall, the patterns observed in this study support *C. hirtus* as a promising bioindicator for freshwater environments impacted by HMs and metal-oxide NPs. Its clear sensitivity to Cu, Cd, and Zn, together with measurable responses to ZnO and CuO, demonstrates that this ciliate can detect contamination across a broad range of metallic forms while remaining robust and easy to handle under laboratory conditions. A key strength of *C. hirtus* lies in its coherent biomarker profile: both non-enzymatic and enzymatic antioxidant parameters respond in a dose-dependent fashion and become strongly coordinated under mixture exposure, providing a sensitive and mechanistically informative readout of oxidative stress. Importantly, *C. hirtus* is able to discriminate between different types of mixture interactions, exhibiting antagonism in Cd + Zn and pronounced synergism in Cd + ZnO. This ability to reflect not only toxicity levels but also the interactive behavior of co-occurring contaminants is particularly relevant for modern ecotoxicology, where organisms are seldom exposed to single chemicals in isolation. Finally, ecological traits such as cosmopolitan distribution and a broad trophic spectrum enhance the relevance of *C. hirtus* as a model organism capable of linking controlled laboratory assays with realistic exposure pathways in natural freshwater systems. Taken together, these characteristics indicate that *C. hirtus* could be effectively integrated into ecotoxicological test batteries and biomonitoring programs aimed at assessing the combined impacts of HMs and metal-based nanomaterials. Continued research involving longer exposure durations, additional biological endpoints, and more complex contaminant mixtures will further refine its applicability as a bioindicator species.

5. Conclusions

This study provides the first quantitative assessment of how *C. hirtus* responds to HMs and metal-oxide NPs through both acute toxicity and antioxidant biomarkers. The species displayed distinct sensitivity patterns across contaminants, with clear differentiation between the effects of dissolved metals and nanoparticulate forms. Mixture experiments highlighted that the nature of chemical interactions depends strongly on contaminant speciation, with antagonism characterizing Cd + Zn and pronounced synergism occurring in Cd + ZnO. These findings emphasize the necessity of including mixture scenarios in ecotoxicological evaluations, particularly when emerging nanomaterials co-occur with traditional metal pollutants.

At the sub-lethal level, *C. hirtus* exhibited consistent modulation of antioxidant defenses, confirming that biochemical indicators provide an effective early-warning signal of metal-induced oxidative stress. The combination of sensitivity, measurable biomarker responses, and ecological relevance supports the use of *C. hirtus* as a suitable candidate for integration into freshwater ecotoxicity testing and biomonitoring strategies. Further studies incorporating longer exposures, additional biological endpoints, and more complex environmental mixtures will strengthen the applicability of *C. hirtus* as a bioindicator and refine its role within integrated assessment frameworks for metallic and nanomaterial contamination.

Author Contributions: Conceptualization, A.L.T.; Methodology, G.R.V., A.G., S.S. and A.L.T.; Software, G.R.V. and F.D.; Validation, G.R.V., F.D., D.B., S.K., M.C. and A.L.T.; Formal analysis, G.R.V., A.L.T. and F.D.; Investigation, G.R.V., A.L.T., S.K., D.B., A.G. and S.S.; Resources, F.D., A.C.K., S.K. and A.L.T.; Data Curation, G.R.V., A.L.T. and F.D.; Writing—Original Draft Preparation, G.R.V. and A.L.T.; Writing—Review and Editing F.D., D.B., S.K., M.C., A.G., A.C.K., S.S. and A.L.T.; Visualization A.L.T. and M.C.; Supervision, A.L.T.; Project Administration, A.L.T.; Funding Acquisition, A.L.T. All authors have read and agreed to the published version of the manuscript.

Funding: This work was supported by the 2017 FFABR—"Fund for Financing Basic Research Activities"—of the Italian Ministry of Education (BVI120008) to A.L.T.

Institutional Review Board Statement: Not applicable.

 doi:10.20944/preprints202512.1836.v1

Informed Consent Statement: Not applicable.

Data Availability Statement: The original contributions presented in this study are included in the article. Further inquiries can be directed to the corresponding author.

Conflicts of Interest: The authors declare no conflicts of interest.

References

1. Mosleh, Y.Y.; Paris-Palacios, S.; Biagianti-Risbourg, S. Metallothioneins induction and antioxidative response in aquatic worms Tubifex tubifex (Oligochaeta, Tubificidae) exposed to copper. Chemosphere 2006, 64, 121-128.
2. Farkas, J.; Peter, H.; Ciesielski, T.M.; Thomas, K.V.; Sommaruga, R.; Salvenmoser, W.; Weyhenmeyer, G.A.; Tranvik, L.J.; Jenssen, B.M. Impact of TiO 2 nanoparticles on freshwater bacteria from three Swedish lakes. Science of The Total Environment 2015, 535, 85-93.
3. Seebaugh, D.R.; Goto, D.; Wallace, W.G. Bioenhancement of cadmium transfer along a multi-level food chain. Marine environmental research 2005, 59, 473-491.
4. Vardakas P., Kyriazis I.D., Kourti M., Skaperda Z., Tekos F., Kouretas D. Chapter 6 - Oxidative stress–mediated nanotoxicity: mechanisms, adverse effects, and oxidative potential of engineered nanomaterials. Advanced Nanomaterials and Their Applications in Renewable Energy (Second Edition), Elsevier, 2022, Pages 179-218, ISBN 9780323998772. https://doi.org/10.1016/B978-0-323-99877-2.00012-6
5. Uddin, M. N., Desai, F., & Asmatulu, E. Engineered nanomaterials in the environment: bioaccumulation, biomagnification and biotransformation. Environmental Chemistry Letters, 2020, 18(4), 1073-1083. https://doi.org/10.1007/s10311-019-00947-0
6. Kabir, E., Kumar, V., Kim, K. H., Yip, A. C., & Sohn, J. R. Environmental impacts of nanomaterials. Journal of Environmental Management, 2018, 225, 261-271. https://doi.org/10.1016/j.jenvman.2018.07.087
7. Zhao, Y., Wang, Y., Wang, X., & Fan, W. Metal-based nanoparticles in natural aquatic environments: concentrations, toxic effects and kinetic processes. Aquatic Toxicology, 2025, 107454. https://doi.org/10.1016/j.aquatox.2025.107454
8. Ale, A., Andrade, V. S., Gutierrez, M. F., Ayech, A., Monserrat, J. M., Desimone, M. F., & Cazenave, J. Metal-based nanomaterials in aquatic environments: What do we know so far about their ecotoxicity? Aquatic Toxicology, 2024, 275, 107069. https://doi.org/10.1016/j.aquatox.2024.107069
9. Peng, C., Zhang, W., Gao, H., Li, Y., Tong, X., Li, K., ... & Chen, Y. Behavior and potential impacts of metal-based engineered nanoparticles in aquatic environments. Nanomaterials, 2017, 7(1), 21. https://doi.org/10.3390/nano7010021
10. Varatharajan, G. R., Calisi, A., Kumar, S., Bharti, D., Ghosh, A., Singh, S., Kharkwal A.C., Coletta M., Dondero F. & La Terza, A. Heavy Metals Affect the Antioxidant Defences in the Soil Ciliate Rigidohymena tetracirrata. Journal of Xenobiotics, 2025,15(5), 169. https://doi.org/10.3390/jox15050169
11. Van Beelen, P.; Doelman, P. Significance and application of microbial toxicity tests in assessing ecotoxicological risks of contaminants in soil and sediment. Chemosphere 1997, 34, 455-499.
12. Foissner, W. Soil protozoa as bioindicators: pros and cons, methods, diversity, representative examples. Agriculture, Ecosystems & Environment 1999, 74(71), 95-112.
13. Madoni, P.; Romeo, M.G. Acute toxicity of heavy metals towards freshwater ciliated protists. Environmental Pollution 2006, 141(141), 141-147.
14. Martín-González, A., Díaz, S., Borniquel, S., Gallego, A., & Gutiérrez, J. C. Cytotoxicity and bioaccumulation of heavy metals by ciliated protozoa isolated from urban wastewater treatment plants. Research in microbiology 2006, 157(152), 108-118.
15. Kim, S.H., Kim, S. J., Lee, J. S., & Lee, Y. M. Acute effects of heavy metals on the expression of glutathione-related antioxidant genes in the marine ciliate Euplotes crassus. Marine pollution bulletin 2014, 85(82), 455-462.
16. Zou, X.Y., Xu, B., Yu, C. P., & Zhang, H. W. Combined toxicity of ferroferric oxide nanoparticles and arsenic to the ciliated protozoa Tetrahymena pyriformis. Aquatic toxicology 2013, 134, 166-173.

 doi:10.20944/preprints202512.1836.v1

17. Yang, W.-W.; Wang, Y.; Huang, B.; Wang, N.-X.; Wei, Z.-B.; Luo, J.; Miao, A.-J.; Yang, L.-Y. TiO2 nanoparticles act as a carrier of Cd bioaccumulation in the ciliate Tetrahymena thermophila. Environmental science & technology 2014, 48, 7568-7575.
18. Gomiero, A., Dagnino, A., Nasci, C., & Viarengo, A. The use of protozoa in ecotoxicology: application of multiple endpoint tests of the ciliate E. crassus for the evaluation of sediment quality in coastal marine ecosystems. Science of the Total Environment 2013, 442, 534-544.
19. Pudpong, S.; Chantangsi, C. Effects of Four Heavy Metals on Cell Morphology and Survival Rate of the Ciliate Bresslauides sp. Tropical Natural History 2015, 15, 117–125.
20. Kim Se-Hun, M.-Y.J., & Young-Mi Lee. Effect of heavy metals on the antioxidant enzymes in the marine ciliate Euplotes crassus. Toxicology and Environmental Health Sciences 2011, 3(4): 213-219.
21. Foissner, W; Berger, H; Schaumburg, J. Identification and ecology of limnetic plankton ciliates. Informationsberichte des Bayerischen Landesamtes für Wasserwirtschaft 1999, 3/99, 1-793.
22. Pfister, G; Auer, B; Arndt, H. Community analysis of pelagic ciliates in numerous different freshwater and brackish water habitats. Verhandlungen der Internationalen Vereinigung für Theoretische und Angewandte Limnologie 2002, 27, 3404-3408.
23. Mazanec, A; Trevarrow, B. Coleps, scourge of the baby Zebrafish. The Zebrafish Science Monitor 1998, 5, 1.
24. Bharti, D; Kumar, S; Buonanno, F; Ortenzi, C; Montanari, A; Quintela-Alonso, P; La Terza, A. Free living ciliated protists from the chemoautotrophic cave ecosystem of Frasassi (Italy). Subterranean Biology 2022, 44, 167-198.
25. Foissner, W. Infraciliatur, Silberliniensystem und Biometrie einiger neuer und wenig bekannter terrestrischer, limnischer und mariner Ciliaten (Protozoa: Ciliophora) aus den Klassen Kinetofragminophora, Colpodea und Polyhymenophora. Stapfia 1984, 12, 1-165.
26. Sleigh, M. Protozoa and other protists. Edward Arnold, London. 1989.
27. Pinto, E.; Sigaud-kutner, T.; Leitao, M.A.; Okamoto, O.K.; Morse, D.; Colepicolo, P. Heavy metal–induced oxidative stress in algae. Journal of Phycology 2003, 39, 1008-1018.
28. Kim, S.-H.; Jung, M.-Y.; Lee, Y.-M. Effect of heavy metals on the antioxidant enzymes in the marine ciliate Euplotes crassus. Toxicology and Environmental Health Sciences 2011, 3, 213-219.
29. Rico, D.; Martín-González, A.; Díaz, S.; de Lucas, P.; Gutiérrez, J.-C. Heavy metals generate reactive oxygen species in terrestrial and aquatic ciliated protozoa. Comparative Biochemistry and Physiology Part C: Toxicology & Pharmacology 2009, 149, 90-96.
30. Valko, M.; Morris, H.; Cronin, M. Metals, toxicity and oxidative stress. Current medicinal chemistry 2005, 12, 1161-1208.
31. Leonard, S.S., Jacquelyn J. Bower, and Xianglin Shi. Metal-induced toxicity, carcinogenesis, mechanisms and cellular responses. Molecular and cellular biochemistry 2004, 255(251): 253-210.
32. Lister, K.N.; Lamare, M.D.; Burritt, D.J. Oxidative Damage in Response to Natural Levels of UV-B Radiation in Larvae of the Tropical Sea Urchin Tripneustes gratilla. Photochemistry and photobiology 2010, 86, 1091-1098.
33. Zhang Ying, J.S., Huamao Yuan, Yayan Xu, and Zhipeng He. Concentrations of cadmium and zinc in seawater of Bohai Bay and their effects on biomarker responses in the bivalve Chlamys farreri. Archives of environmental contamination and toxicology 2010, 59(51): 120-128.
34. Kim, R.-O., Jae-Sung Rhee, Eun-Ji Won, Kyun-Woo Lee, Chang-Mo Kang, Young-Mi Lee, and Jae-Seong Lee. Ultraviolet B retards growth, induces oxidative stress, and modulates DNA repair-related gene and heat shock protein gene expression in the monogonont rotifer, Brachionus sp. Aquatic Toxicology 2011, 101(103): 529-539.
35. Rehman, A.; Shakoori, F.R.; Shakoori, A.R. Heavy metal resistant freshwater ciliate, Euplotes mutabilis, isolated from industrial effluents has potential to decontaminate wastewater of toxic metals. Bioresource technology 2008, 99, 3890-3895.
36. Gomiero, A.; Dagnino, A.; Nasci, C.; Viarengo, A. The use of protozoa in ecotoxicology: application of multiple endpoint tests of the ciliate E. crassus for the evaluation of sediment quality in coastal marine ecosystems. Science of the Total Environment 2013, 442, 534-544.

 doi:10.20944/preprints202512.1836.v1

37. Kim, S.-H.; Kim, S.-J.; Lee, J.-S.; Lee, Y.-M. Acute effects of heavy metals on the expression of glutathione-related antioxidant genes in the marine ciliate Euplotes crassus. Marine pollution bulletin 2014, 85, 455-462.
38. Mori, G.; Erra, F.; Cionini, K.; Banchetti, R. Sublethal doses of heavy metals and Slow-Down pattern of Euplotes crassus (Ciliophora, Hypotrichia): A behavioural bioassay. Italian Journal of Zoology 2003, 70, 23-30.
39. Jonker, M.J.; Svendsen, C.; Bedaux, J.J.; Bongers, M.; Kammenga, J.E. Significance testing of synergistic/antagonistic, dose level-dependent, or dose ratio-dependent effects in mixture dose-response analysis. Environmental Toxicology and Chemistry: An International Journal 2005, 24, 2701-2713.
40. Miyake, A. Physiology and biochemistry of conjugation in ciliates. Biochemistry and physiology of protozoa 1981, 4, 125-198.
41. Clark, C.; Lee, J.; Soldo, A. Protocols in protozoology. Lee JJ, Soldo A., editors 1992, 1, D3.
42. Brunelli, A., Cazzagon, V., Faraggiana, E., Bettiol, C., Picone, M., Marcomini, A., & Badetti, E. An overview on dispersion procedures and testing methods for the ecotoxicity testing of nanomaterials in the marine environment. Science of the Total Environment, 2024, 921, 171132.
43. Strober, W. Trypan blue exclusion test of cell viability. Curr. Protoc. Immunol. 2015, 111, A3. B. 1–A3. B. 3.
44. Sprague, J.B. Measurement of pollutant toxicity to fish. II. Utilizing and applying bioassay results. Water Res. 1970, 4, 3–32.
45. Ravindran, C.; Varatharajan, G.R.; Rajasabapathy, R.; Vijayakanth, S.; Kumar, A.H.; Meena, R.M. A role for antioxidants in acclimation of marine derived pathogenic fungus (NIOCC 1) to salt stress. Microbial pathogenesis 2012, 53, 168-179.
46. Vattem, D.A.; Shetty, K. Solid-state production of phenolic antioxidants from cranberry pomace by Rhizopus oligosporus. Food Biotechnology 2002, 16, 189-210.
47. Yıldırım, A.; Mavi, A.; Kara, A.A. Determination of antioxidant and antimicrobial activities of Rumex crispus L. extracts. Journal of agricultural and food chemistry 2001, 49, 4083-4089.
48. Kunchandy, E.; Rao, M. Oxygen radical scavenging activity of curcumin. International journal of pharmaceutics 1990, 58, 237-240.
49. Beers, R.F.; Sizer, I.W. A spectrophotometric method for measuring the breakdown of hydrogen peroxide by catalase. Journal of biological chemistry 1952, 195, 133-140.
50. Mannervik, B.; Alin, P.; Guthenberg, C.; Jensson, H.; Tahir, M.K.; Warholm, M.; Jörnvall, H. Identification of three classes of cytosolic glutathione transferase common to several mammalian species: correlation between structural data and enzymatic properties. Proceedings of the National Academy of Sciences 1985, 82, 7202-7206.
51. Beyer, W.F.; Fridovich, I. Assaying for superoxide dismutase activity: some large consequences of minor changes in conditions. Analytical biochemistry 1987, 161, 559-566.
52. Di Rienzo J.A., Casanoves F., Balzarini M.G., Gonzalez L., Tablada M., Robledo C.W. InfoStat versión 2012. Grupo InfoStat, 2012 Facultad de Ciencias Agropecuarias, Universidad Nacional de Córdoba, Argentina. URL http://www.infostat.com.ar.
53. Chung, K. T., Wong, T. Y., Wei, C. I., Huang, Y. W., & Lin, Y. Tannins and human health: a review. Critical reviews in food science and nutrition, 1998, 38(6), 421-464.
54. Hayyan, M.; Hashim, M.A.; AlNashef, I.M. Superoxide ion: Generation and chemical implications. Chemical reviews 2016, 116, 3029-3085.
55. Varatharajan, G.R.; Calisi, A.; Kumar, S.; Bharti, D.; Dondero, F.; La Terza, A. Cytotoxicity and Antioxidant Defences in Euplotes aediculatus Exposed to Single and Binary Mixtures of Heavy Metals and Nanoparticles. Applied Sciences 2024, 14, 5058.
56. Martín-González, A.; Díaz, S.; Borniquel, S.; Gallego, A.; Gutiérrez, J.C. Cytotoxicity and bioaccumulation of heavy metals by ciliated protozoa isolated from urban wastewater treatment plants. Research in microbiology 2006, 157, 108-118.
57. Mortimer, M.; Kasemets, K.; Kahru, A. Toxicity of ZnO and CuO nanoparticles to ciliated protozoa Tetrahymena thermophila. Toxicology 2010, 269, 182-189.
58. Díaz, S.; Martín-González, A.; Gutiérrez, J.C. Evaluation of heavy metal acute toxicity and bioaccumulation in soil ciliated protozoa. Environment international 2006, 32, 711-717.

 doi:10.20944/preprints202512.1836.v1

59. Blinova, I.; Ivask, A.; Heinlaan, M.; Mortimer, M.; Kahru, A. Ecotoxicity of nanoparticles of CuO and ZnO in natural water. Environmental Pollution 2010, 158, 41-47.
60. Glynn, A.W. The influence of zinc on apical uptake of cadmium in the gills and cadmium influx to the circulatory system in zebrafish (Danio rerio). Comparative Biochemistry and Physiology Part C: Toxicology & Pharmacology 2001, 128, 165-172.
61. Barata, C.; Markich, S.J.; Baird, D.J.; Taylor, G.; Soares, A.M. Genetic variability in sublethal tolerance to mixtures of cadmium and zinc in clones of Daphnia magna Straus. Aquatic Toxicology 2002, 60, 85-99.
62. Fargašová, A. Winter third-to fourth-instar larvae of Chironomus plumosus as bioassay tools for assessment of acute toxicity of metals and their binary combinations. Ecotoxicology and Environmental Safety 2001, 48, 1-5.
63. Rainbow, P.; Amiard-Triquet, C.; Amiard, J.; Smith, B.; Langston, W. Observations on the interaction of zinc and cadmium uptake rates in crustaceans (amphipods and crabs) from coastal sites in UK and France differentially enriched with trace metals. Aquatic Toxicology 2000, 50, 189-204.
64. Sunda, W.G.; Huntsman, S.A. Antagonisms between cadmium and zinc toxicity and manganese limitation in a coastal diatom. Limnology and Oceanography 1996, 41, 373-387.
65. González-Párraga, P.; Hernández, J.A.; Argüelles, J.C. Role of antioxidant enzymatic defences against oxidative stress (H2O2) and the acquisition of oxidative tolerance in Candida albicans. Yeast 2003, 20, 1161-1169.
66. Estruch, F. Stress-controlled transcription factors, stress-induced genes and stress tolerance in budding yeast. FEMS microbiology reviews 2000, 24, 469-486.
67. Shakoori, F.R.; Zafar, M.F.; Fatehullah, A.; Rehman, A.; Shakoori, A. Response of Glutathione Level in a Protozoan Ciliate, Stylonychia mytilus, to increasing uptake of and Tolerance to Nickel and Zinc in the Medium. J. Zool 2011, 43, 569-574.
68. Amaretti, A.; Di Nunzio, M.; Pompei, A.; Raimondi, S.; Rossi, M.; Bordoni, A. Antioxidant properties of potentially probiotic bacteria: in vitro and in vivo activities. Applied microbiology and biotechnology 2013, 97, 809-817.
69. Fırat, Ö.; Cogun, H.Y.; Aslanyavrusu, S.; Kargın, F. Antioxidant responses and metal accumulation in tissues of Nile tilapia Oreochromis niloticus under Zn, Cd and Zn+ Cd exposures. Journal of Applied Toxicology 2009, 29, 295-301.